Modeling COVID-19 dynamics in the sixteen West African countries

Sewanou H. Honfo[1], Hémaho B. Taboe[1], Romain Glèlè Kakaï[1*]

[1] Laboratoire de Biomathématiques et d'Estimations Forestières, Université d'Abomey-Calavi, Benin

* romain.glelekakai@fsa.uac.bj

Abstract

The current COVID-19 pandemic has caused several damages to the world, especially in public health sector. This study considered a simple deterministic SIR (Susceptible-Infectious-Recovered) model to characterize and predict future course of the pandemic in the West African countries. We estimated specific characteristics of the disease's dynamics such as its initial conditions, reproduction numbers, true peak, reported peak with their corresponding times, final epidemic size and time-varying attack ratio. Our findings revealed a relatively low proportion of susceptible individuals in the region and in the different countries (1.2% across West Africa). The detection rate of the disease was also relatively low (0.9% for West Africa as a whole) and $< 2\%$ for most countries, except for Cape-Verde (9.5%), Mauritania (5.9%) and Ghana (4.4%). The reproduction number varied between 1.15 (Burkina-Faso) and 4.45 (Niger) and the peak time of the pandemic was between June and July for most countries. Most generally, the reported peak time came a week (7-8 days) after the true peak time. The model predicted $222,100$ actual active cases in the region at peak time while the final epidemic size accounted for 0.6% of the West African population ($2,526,700$ individuals). Results obtained showed that the COVID-19 pandemic has not severely affected West Africa as noticed in other regions of the world, but current control measures and standard

operating procedures should be maintained over time to ensure trends observed and even accelerate the declining trend of the pandemic.

Keywords: COVID-19, detection rate, peak time and size, final epidemic size, attack ratio, Africa

Introduction

The COVID-19 pandemic is a severe acute respiratory syndrome caused by the new coronavirus, SARS-CoV-2, which has emerged from Wuhan, Hubei Province (China) in the last days of 2019 [25, 39]. It is currently the most important threat to global public health . By August 15th, 2020, about 21,026,758 total confirmed cases and 755,786 deaths were recorded worldwide [44]. The disease was rapidly spread around the world (about 212 countries) [27] including the 54 African countries. By mid August 2020, The World Health Organisation (WHO) reported 936,062 and 152,483 confirmed cases and 18,286 and 2,351 deaths across Africa and the West-African region, respectively [44]. Healthcare services in the region have particularly faced critical time sensitive decisions regarding patients and their treatment [28]. It is clear that the COVID-19 pandemic has severely affected people's life, health and economy. Actually, it led to an important increase in the demand of hospital beds and artificial respirators (mechanic and non-invasive). According to the WHO global health observatory data, most countries in West Africa have less than 5 hospital beds and 2 medical doctors per 10,000 of the population, while 50% of the countries have health expenditures lower than US$50 per capita [46]. In contrast, European countries such as Italy and Spain, 34 and 35 hospital beds, respectively, per 10,000 of the population are noted, 41 medical doctors per 10,000 of the population, and US$2,840 and US$2,506 per capita expenditure [34]. Moreover, medical staff in the World were directly exposed to infections [26]. Since vaccines are still under development, and antiviral drugs are not available for effective curative treatment of COVID-19 infections, the actual cure practice is hospitalization and intensive care unit management [32]. Prevention measures used are essentially non-pharmaceutical interventions such as regular hand washing with soap, mask wearing and social distancing. To be efficient, these non-pharmaceutical measures required a good understanding of the dynamic of the spread of the disease.

Mathematical and statistical models can be extremely helpful tools to make decisions in public health. They are also important to ensure optimal use of resources to reduce the morbidity and mortality associated with epidemics, through estimation and prediction [27–30,33]. The prediction of essential epidemiological parameters such as the peak time, the duration and the final size of the outbreak is crucial and important for policy makers and public health authorities to make appropriate decisions for the control of the pandemic [32]. Therefore, modelling and forecasting the numbers of confirmed and recovered COVID-19 cases play an important role in designing better strategies for the control of the COVID-19's spread in the world [27, 29]. Since the appearance of the first COVID-19 case in the world, several studies have been conducted to model the dynamics of the disease. The main methods used were: deterministic modelling techniques (SIR, eSIR, SEIR, SEIRD, etc. compartmental models) [24,29,30,33,41–43], autoregressive time series models based on two-piece scale mixture normal distributions [27], stochastic modelling methods [49, 50], machine learning techniques [47, 48], growth models [43, 52, 53] and bayesian method [48].

Among these modeling techniques, deterministic models are the most considered because of their simplicity. However, they fail to provide accurate results due to non-identifiability problem when the number of compartments and the number of parameters are high [39]. Actually, complex deterministic models have been showed to be less reliable than simpler model such as SIR model framework [39], which performs better in describing trends in epidemiological data. This under-performance may be worse when meta-population confirmed-cases data are considered. However, only few studies related to COVID-19 in Africa used mathematical models and prevalence data to study the dynamics, analyze the causes and key factors of the outbreak [24, 25, 51]. Recently, [24] assessed the current pattern of COVID-19 spread in West Africa using a deterministic compartmental SEIR-type model.

In this study, we used a simple deterministic SIR model to characterize and predict future trend of the spread of the pandemic in West Africa. Specifically, we aimed to estimate specific characteristics of COVID-19 dynamics (initial conditions of the pandemic, reproduction numbers, true peak, reported peak and their times and dates, final epidemic size and time-varying attack ratio). The originality of this work is that it focuses on the sixteen West African countries and the whole region as well. It is the first

study dealing with the dynamic of the pandemic in each of the West African countries.

Methods

Model description

Problems of non-identifiability in parameters estimation in deterministic compartment models (especially complex models) are common in epidemiological modelling studies, which often imply biased estimations of parameters. [39] recommended the use of simpler models which overperformed complex models in estimating reliable parameters. Hence, in this study, the simple SIR model [31] was considered with the particularity of two removal rates and illustrated in the system below [17]:

$$\begin{cases} \dfrac{dS}{dt} = -\dfrac{\beta SI}{N} \quad ; \quad N = S + I + R, \\ \dfrac{dI}{dt} = \dfrac{\beta SI}{N} - (\nu_1 + \nu_2)I, \\ \dfrac{dR}{dt} = (\nu_1 + \nu_2)I, \end{cases} \tag{1}$$

with initial conditions,

$$\begin{cases} S(0) = S_0 > 0 \\ I(0) = I_0 > 0 \\ R(0) = R_0 \geq 0 \\ N(0) = N = S_0 + I_0 + R_0. \end{cases}$$

In (1), $S = S(t)$, $I = I(t)$ and $R = R(t)$ represent the number of susceptible, infected and removed individuals at time t, respectively while N is defined as the total population size for the disease transmission. The parameters β, ν_1 and ν_2 are the transmission rate, the removal rate of reported infected individuals (detected) and the removal rate of infected individuals due to all other unreported causes (mortality, recovery or other reasons), respectively. We considered the removal rate ν_2 as constant with value $\nu_2 = 1/10$ [54]. From the second differential equation of (1), one can notice that $\nu_1 I_0$ represents the daily confirmed cases (Ir_0) at time 0 of the outbreak. Thus, the relationship between the initial number of infected individuals and the detection rate, ν_1 is as follow and used in the estimation process:

$$I_0 = I r_0 / \nu_1.$$

Data consideration and parameter estimation procedure

For each country, the data considered for the modeling spans the period from the date of detection of the first case of COVID-19 in the country and August, 12, 2020. Data considered were the daily numbers of reported cases that have been assimilated to $\nu_1 I$. These data were downloaded from the Global Rise of Education website [55]. Table 1 presents the demographic patterns [11], initial dates of the pandemic [55] and testing efforts (identification of new cases) of the countries [11]. We fitted the model (1) to the observed daily cases to study the dynamics of COVID-19 pandemic in the sixteen West African countries.

To improve the prediction power of (1), we used a cross-validation procedure of parameter estimation, where 90% of the observations were considered to estimate values of the six unknown model parameters $(S_0, I_0, R_0, \beta, \nu_1, \nu_2)$ and the remaining observations were used to validate the model. The Root Mean Square Error (RMSE) statistics was used as the measure of estimation precision:

$$RMSE = \sqrt{\frac{\sum_{r=1}^{k} (\hat{\theta} - \theta)^2}{k}}, \tag{2}$$

where $\hat{\theta}$ and θ are the predicted and observed number of daily cases respectively; k is the number of observations considered. We considered as $RMSE_1$, the Root Mean Square Error computed on the 90% of the observations and $RMSE_2$, computed on the remaining observations (10%)

The solutions of (1) were obtained using the built-in function *ODE45* of Matlab [56]. Then, the non linear least square estimate technique was performed to estimate the six parameters in (1) given starting values, using the built-in function *fminsearchbnd* of Matlab [56].

Afterwards, we simulated 2,000 different starting values of the six parameters using a resampling method (function *resample* of Matlab) for S_0, I_0 and R_0 and the uniform distribution (function *rand* of Matlab) for β and ν_1. Then, we estimated for each of the starting points, values of the six parameters using the non-linear least square technique described above. The final values considered for the these parameters are those related

to both smallest values of $RMSE_2$ and $RMSE_1$ to guarantee a good fit of the model and a good predictive power. At the end of this process, we obtained reliable estimates of the model parameters with 95 % confidence intervals. Curves were plotted to show evolution trends of predicted daily new COVID-19, daily reported cases and the attack ratio for the 16 countries. With the estimated values of the six parameters from (1), the COVID-19 dynamic in each country was characterized computing the following parameters with their 95% confidence intervals. Table 1 presents demographic patterns and testing efforts in the West African region.

Table 1. Demographic patterns and testing efforts of the 16 West African countries

Countries	Population size	Density	First case	Tests/1M Pop	Cases/1000 tests
Benin	12,123,200	108	03/16/2020	9,711	18
Burkina-Faso	20,946,992	76	03/10/2020	-	-
Cape-verde	556,498	138	03/21/2020	137,485	50
Côte d'Ivoire	26,428,999	83	03/12/2020	4,779	142
Gambia	2,421,823	239	03/17/2020	5,502	222
Ghana	31,072,945	137	03/12/2020	14,183	100
Guinea	13,160,021	53	03/14/2020	1,860	382
Guinea-Bissau	1,971,640	70	03/25/2020	-	-
Liberia	5,066,990	53	03/16/2020	-	-
Mali	20,294,900	17	03/26/2020	1,852	74
Mauritania	4,659,052	5	03/15/2020	14,980	100
Niger	24,269,389	19	03/22/2020	372	130
Nigeria	206,522,290	226	02/28/2020	1,943	134
Senegal	16,776,618	87	03/02/2020	8,632	93
Sierra-Leone	7,989,949	111	04/01/2020	-	-
Togo	8,293,924	152	03/07/2020	7,784	22
West Africa	402,555,230	66	02/28/2020	-	-

Date: 08/31/2020; Source: [11] and [55]; Tests/1M Pop: number of tests per 1 million individuals; Cases/1000 tests: number of positive cases per 1000 tests; - : no data.

- *Reproduction number*, $\mathscr{R}_0$ $[1, 16]$: It is the average number of new cases of infec-

tion, caused by an average infected individual (during his infectious period), in a fully constituted population:

$$\mathscr{R}_0 = \frac{\beta}{\nu_1 + \nu_2}. \tag{3}$$

- *Running reproductive number*, $\mathscr{R}_e$ [1]: measures the number of secondary infections caused by a single infected individual in the population at time t.

$$\mathscr{R}_e = \frac{S(t)}{N}\frac{\beta}{\nu_1 + \nu_2}. \tag{4}$$

- *True peak size*, n_{pp} and *True peak time*, T_{pp}. The true peak size indicates the largest daily number of new infectious cases in the population:

$$n_{pp} = max(\beta\frac{SI}{N}),$$

while the true peak time, T_{pp} represents the time at which the largest daily new infected cases is obtained. These two parameters were determined numerically.

- *Reported peak size*, n_{rp} and *Reported peak time*, T_{rp}. The reported peak size indicates the largest number of daily reported cases:

$$n_{rp} = max(\nu_1 I),$$

while the reported peak time is the associated time to n_{rp}. They were determined numerically.

- *Maximum number of active cases*, I_{max}: since $I_0, R_0 << S_0$, we assumed the number of initial susceptible individuals to be approximately equal to N ($S_0 \approx N$). Thus, I_{max} can be approximated as follow [16]:

$$I_{max} \approx N\left[1 - \frac{1}{\mathscr{R}_0}(1 + log(\mathscr{R}_0))\right]. \tag{5}$$

- *Final epidemic size*, I_{total} [16]: it is the total number of cases over the course of the epidemic wave.

$$I_{total} = S_0 - S_\infty; \quad S_\infty = lim_{t\to\infty}S(t). \tag{6}$$

S_∞ can be approximated considering the entire population as initially susceptible ($S_0 \approx N$); hence, following [16]:

$$log\left(\frac{S_\infty}{N}\right) = \mathscr{R}_0\left(\frac{S_\infty}{N} - 1\right). \tag{7}$$

For each country, the equation (7) was solved numerically to determine S_∞ through an iterative process.

- *Attack ratio*, A_r [17]: is the fraction of susceptible population that becomes infected. It is calculated along the epidemic wave as follow:

$$\begin{aligned} A_r(t) &= \frac{S_0 + I_0 + R_0 - S(t)}{S_0 + I_0 + R_0} \\ &= \frac{N - S(t)}{N}. \end{aligned} \tag{8}$$

For the West Africa as a whole, S_0, I_0 and R_0 were first computed by summing the corresponding estimated values of the 16 countries. Afterwards, the model (1) was fitted to daily reported cases of the region using initial conditions computed. This allowed the estimation of β and ν_1 and computation of the characteristics of COVID-19 dynamics across the region.

Results

Current patterns of COVID-19 transmission in West Africa

Table 1 reveals a great heterogeneity in the region in terms of population density and testing efforts. Countries like Cape-Verde, Mauritania and Ghana have put relatively more effort into identifying infected individuals while Niger, Nigeria and Guinea are countries with the lowest number of tests per 1 million people. Combining both the testing effort and the mean number of reported cases per test indicate a relatively less testing effort to identify many infected individuals (Guinea and Gambia). On the other hand, countries like Cape-Verde, Benin and Togo put much effort to find few COVID-19 cases (Table 1).

Results obtained from the estimation of initial conditions of COVID-19 pandemic in West Africa revealed the relatively low proportion of the susceptible individuals in most countries (about 1% of their total populations). However, countries such as Guinea-Bissau, Gambia and Cape-Verde showed relatively large proportion of susceptible individuals to COVID-19 with 17.5%, 6.0% and 2.4% of their total populations, respectively. The proportion of the susceptible individuals across West Africa was also

relatively low (1.2%) (Tables 1 and 2). Moreover, before the detection of the first cases, infected individuals were present in the population of all the countries with some already recovered individuals. The detection rate of infected individuals was relatively low (less than 1%) for Benin, Burkina, Mali, Niger, Nigeria, Sierra-Leone and West Africa as a whole. However, some countries like Cape-Verde (9.5%) Mauritania (5.9%) and Ghana (4.4%) recorded the highest detection rates, respectively. (Table 3).

In most countries, the model estimated an average of 1 new case of infection caused by an infected individual during his infectious period ($\mathscr{R}_0$) except for Sierra-Leone, Nigeria, and Côte d'Ivoire with $\mathscr{R}_0 \approx 2$ and Niger, which recorded the highest reproduction number ($\mathscr{R}_0 \approx 4$) (Table 3).

Long term dynamics of COVID-19 in West Africa

We analyzed the long term dynamic of COVID-19 in West Africa by first focusing on the true peak of the pandemic. In general, the estimated reported peak time came a week (7-8 days) after the true peak time in all the countries while their estimated reported peak sizes accounted in average for 21% of the estimated true peak size (Table 3). Most countries have already experienced the peak of the epidemic wave. The true peak time was estimated in June for Sierra-Leone (14th), Mauritania (19th), Benin (27th), Côte d'Ivoire (24th) and Ghana (13th), while it was estimated in July for Liberia (4th) and Nigeria (5th), Senegal (18th), Guinea (23th) and Cape-Verde (22th) and October 4th for Togo. Niger recorded the earliest true peak time (April 8th) while the latest true peak time was on December 10th, 2020 for Gambia (Figure 1 and Table 3). The true peak time across the region was July 1st with 25,267 new cases (Table 3 and Figure 4a and 4b). Margin error of the estimated true peak time varies from 1 day to 16 days with average value of 5 days in the region. Half of the countries (8 out of 16) recorded true peak size less than 1000 new cases cases at peak time. The highest numbers of new cases at peak time were estimated at 19,021 and 17,703 for Niger and Nigeria respectively (Table 3 and Figure 1). The estimates of the reported peak size was 1,891 daily cases across the region (Table 3 and Figures 4a-b).

Table 2. Estimates with 95% confidence intervals of the initial parameters of the SIR-model; $\nu_2 = 0.10$ is constant for all countries

Country	S_0 x10^5	I_0	R_0	β	ν_1	**RMSE2**
Benin	1.212 [1.211-1.214]	200 [197-203]	39 [37-40]	0.148 [0.145-0.151]	0.005 [0.004-0.006]	31.7
Burkina-Faso	2.175 [2.145-2.206]	174 [164-183]	160 [149-172]	0.121 [0.121-0.122]	0.006 [0.005-0.007]	8.0
Cape-Verde	0.517 [0.460-0.573]	21 [17-26]	97 [91-102]	0.226 [0.221-0.231]	0.095 [0.092-0.098]	98.8
Côte d'Ivoire	2.643 [1.265-4.021]	73 [23-124]	8 [6-9]	0.178 [0.175-0.181]	0.014 [0.011-0.017]	65.6
Gambia	1.451 [1.374-1.528]	28 [27-28]	29 [26-32]	0.167 [0.164-0.169]	0.036 [0.034-0.039]	78.9
Ghana	3.291 [2.388-4.193]	46 [24-68]	81 [80-83]	0.20 [0.197-0.203]	0.044 [0.041-0.047]	462.0
Guinea	3.789 [3.428-4.151]	229 [206-251]	85 [82-88]	0.146 [0.145-0.148]	0.004 [0.004-0.005]	35.7
Guinea-Bissau	3.458 [3.452-3.497]	1990 [1970-2011]	4 [2-5]	0.146 [0.144-0.147]	0.001 [0.000-0.004]	15.2
Liberia	0.507 [0.506-0.508]	100 [98-102]	87 [85-89]	0.146 [0.143-0.149]	0.010 [0.007-0.013]	153.4
Mali	2.240 [2.215-2.265]	1175 [1139-1211]	199 [194-203]	0.167 [0.165-0.169]	0.002 [0.000-0.005]	39.1
Mauritania	0.466 [0.291-0.641]	17 [8-26]	42 [41-44]	0.221 [0.216-0.225]	0.059 [0.055-0.063]	40.7
Niger	2.427 [1.578-3.276]	1203 [1250-1296]	39 [47-54]	0.448 [0.441-0.455]	0.001 [0.000-0.001]	2.1
Nigeria	20.886 [10.651-31.121]	252 [212-293]	110 [102-117]	0.173 [0.169-0.178]	0.004 [0.000-0.009]	2926.6
Senegal	1.976 [0.723-3.230]	61 [16-138]	99 [98-101]	0.161 [0.160-0.163]	0.016 [0.014-0.019]	48.4
Sierra-Leone	0.799 [0.797-0.801]	200 [191-209]	5 [3-6]	0.166 [0.160-0.171]	0.005 [-0.002-0.012]	7.4
Togo	0.830 [0.662-0.999]	42 [38-45]	28 [26-29]	0.144 [0.143-0.146]	0.024 [0.022-0.026]	8.0
West Africa	48.667 [33.146-64.224]	5811 5580-6214]	1112 [1069-1174]	0.152 [0.151-0.152]	0.009 [0.007-0.010]	1463.3

Table 3. Epidemiological statistics with their 95% confidence intervals indicating the dynamics of COVID-19 in the whole west African region and per country

Country	$\mathscr{R}_0$	$\boldsymbol{T}_{rp}$	$\boldsymbol{n}_{rp}$	$\boldsymbol{T}_{pp}$	$\boldsymbol{n}_{pp}$	$\boldsymbol{I}_{max}$(x10^4)	$\boldsymbol{I}_{total}$ (x10^4)
Benin	1.41 [1.38-1.43]	114 [112-116]	29 [24-34]	104 [103-107]	634 [558-710]	0.57 [0.53-0.61]	6.3 [6.3-6.4]
Burkina-Faso	1.15 [1.14-1.15]	239 [234-245]	12 [11-13]	229 [223-235]	218 [213-222]	0.19 [0.19-0.20]	5.4 [5.3-5.4]
Cape-Verde	1.16 [1.14-1.18]	149 [148-150]	50 [46-53]	144 [143-145]	103 [89-117]	0.05 [0.04-0.06]	1.4 [1.2-1.5]
Côte d'Ivoire	1.56 [1.54-1.58]	113 [112-114]	269 [263-274]	105 [104-106]	2368 [1038-3698]	1.97 [0.73-3.20]	16.4 [7.2-25.6]
Gambia	1.22 [1.22-1.23]	276 [271-281]	921 [851-991]	269 [264-274]	3497 [3351-3643]	2.54 [2.45-2.63]	49.2 [47.2-51.1]
Ghana	1.39 [1.38-1.40]	131 [129-133]	632 [629-634]	124 [123-125]	2138 [1413-2863]	1.44 [0.76-2.13]	16.6 [10.9-22.3]
Guinea	1.40 [1.39-1.41]	141 [139-143]	76 [66-95]	132 [130-134]	1861 [1659-2063]	1.71 [1.53-1.90]	19.3 [18.2-20.5]
Guinea-Bissau	1.44 [1.43-1.46]	83 [82-84]	20 [19-20]	73 [72-74]	2084 [2040-2128]	1.85 [1.81-1.88]	18.7 [18.6-18.9]
Liberia	1.33 [1.32-1.33]	120 [117-125]	17 [17-18]	111 [110-112]	196 [193-198]	0.17 [0.17-0.18]	2.3 [2.2-2.3]
Mali	1.64 [1.63-1.66]	68 [64-72]	35 [34-37]	59 [55-63]	2254 [2189-2320]	2.00 [1.94-2.06]	1.48 [1.47-1.49]
Mauritania	1.39 [1.36-1.42]	103 [101-104]	119 [116-123]	97 [95-99]	331 [243-420]	0.20 [0.05-2.18]	2.3 [2.1-2.5]
Niger	4.45 [4.37-4.52]	20 [12-28]	86 [84-87]	15 [6-24]	19021 [18597-19444]	10.72 [10.49-10.96]	26.2 [20.0-27.9]
Nigeria	1.67 [1.64-1.69]	121 [117-125]	774 [608-824]	112 [108-116]	21800 [6616-36983]	19.50 [11.89-27.11]	141.0 [126.7-249.8]
Senegal	1.38 [1.37-1.39]	147 [146-152]	136 [133-138]	139 [138-140]	989 [55-2033]	0.82 [0.02-1.81]	9.7 [1.8-17.7]
Sierra-Leone	1.58 [1.56-1.60]	83 [78-88]	31 [30-33]	75 [69-81]	700 [673-727]	0.62 [0.59-0.64]	5.0 [4.9-5.2]
Togo	1.16 [1.16-1.17]	220 [218-222]	21 [15-27]	212 [210-214]	110 [100-121]	0.09 [0.08-0.09]	2.2 [2.0-2.4]
West Africa	1.39 [1.38-1.41]	119 [117-121]	1891 [1874-1909]	111 [108-112]	25267 [24239-26294]	22.21 [21.21-23.22]	248.8 [140.8-250.7]

The final epidemic size would account for 0.6% of the population of West Africa. This estimate is generally low ($< 1\%$ of the population size) for more than half of the countries though Gambia, Guinea-Bissau and Cape-Verde would record the highest final epidemic sizes ($> 9\%$ of their populations). The estimates of the maximum number of actual daily active cases at peak time are for most countries greater than 1,000 cases, though, it is $107,200$ and $195,000$ for Niger and Nigeria respectively (Table 3).

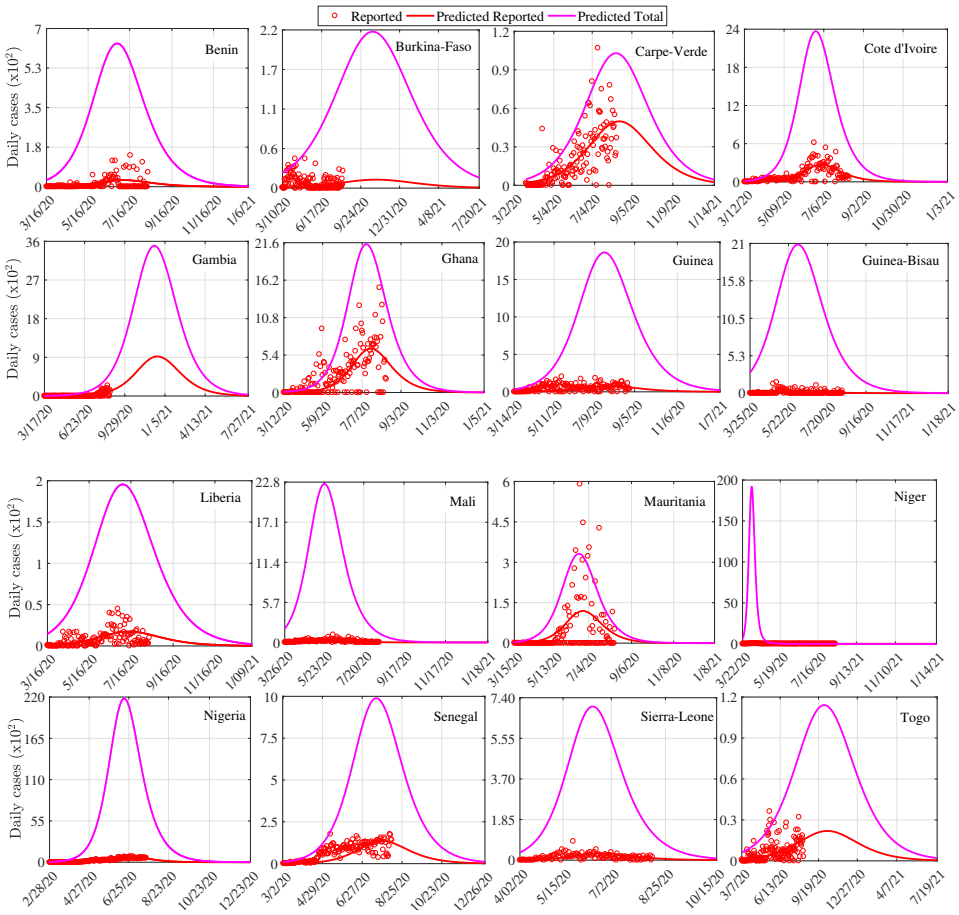

Fig 1. Evolution trend of the COVID-19 daily cases per country.

The running reproduction number helped assess the evolution trend of the disease. It decreased over time in all countries from the beginning of the outbreak ($1.2-4.5$) to a stability point, which varied according to countries ($0.50-0.82$, Figure 2). As expected, the fraction of susceptible individuals being infected (attack ratio) increased over time from 0% to $40\%-70\%$, depending on countries. These evolving trends in reproduction number and attack ratio are similar to those noted for West Africa as a whole (Figure 4b-c).

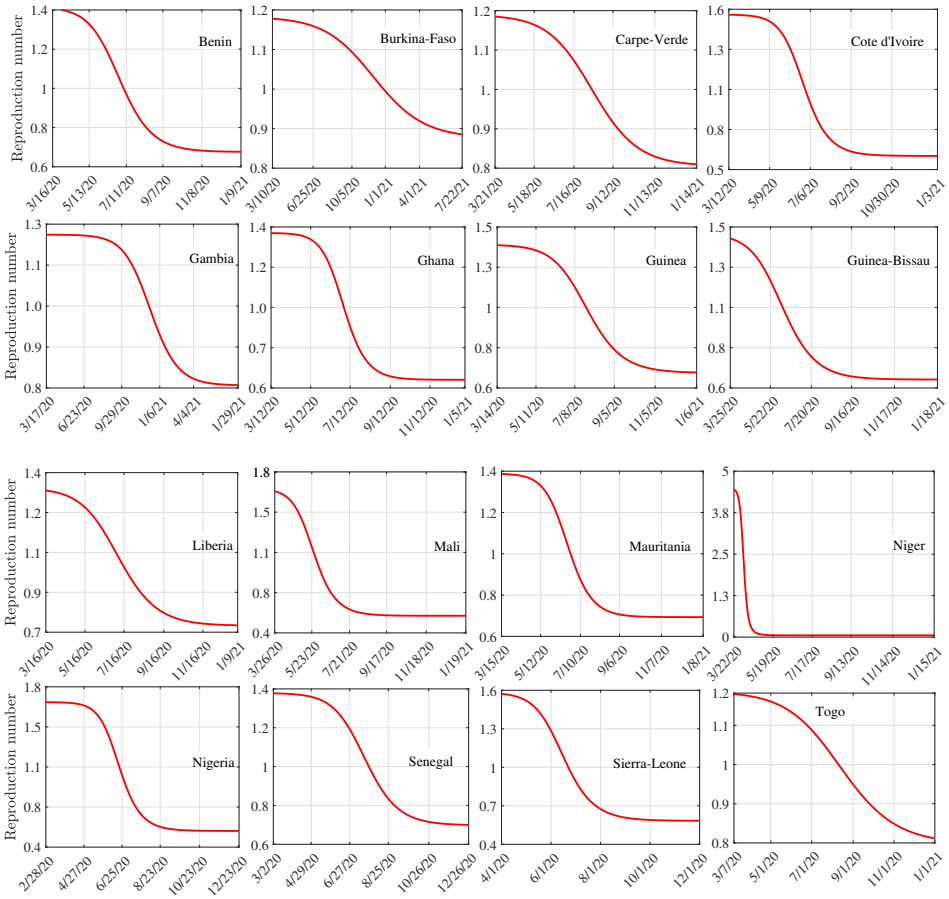

Fig 2. Running reproduction number per country in West Africa.

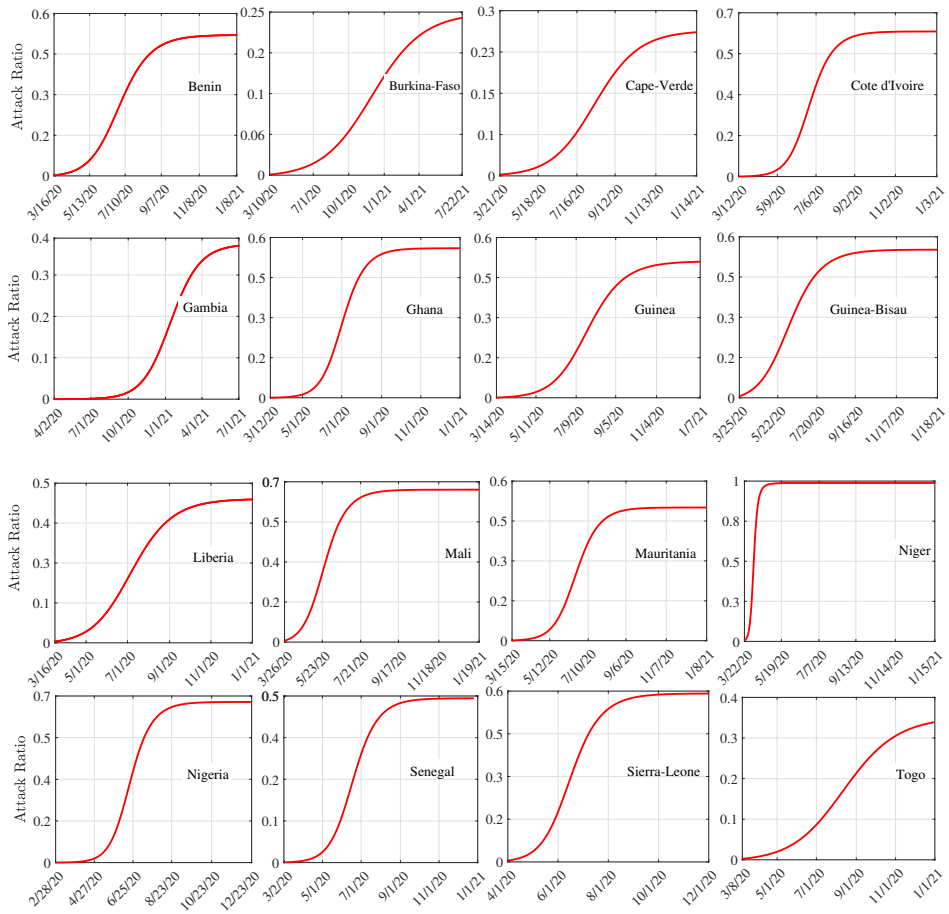

Fig 3. Evolution trend of the attack ratio per country in West Africa.

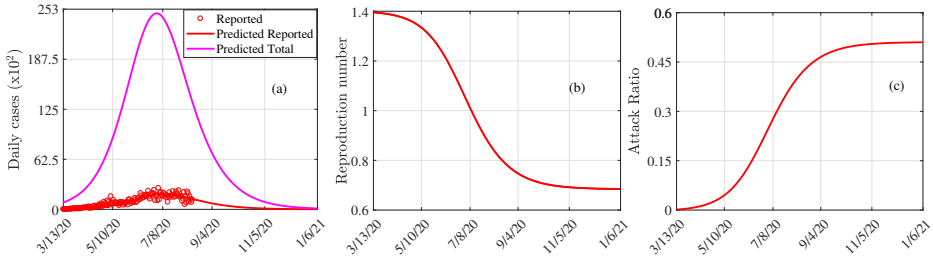

Fig 4. Trend in COVID-19 dynamics across West Africa. (a) Prediction of true peak and reported peak date and size of COVID-19. (b). Evolution trend of the reproduction number. (c) Evolution trend of the attack ratio.

Discussion

In epidemiology, understanding the dynamics of an epidemic outbreak and predicting its future course is a major research question, which is often studied using modelling techniques [2, 18–23]. Estimation and prediction rely on mathematical and statistical models, which inform public health decisions and ensure optimal use of resources to reduce the morbidity and mortality associated with epidemics [14,27–30,33]. For instance, estimation of epidemiological parameters and prediction on the *Influenza* outbreak dynamics in Canada was done using the Richard's model [14], while a three-parameter logistic growth model was used to study and forecast the final epidemic size in real-time of the *Zika* virus outbreaks in Brazil from 2015 to 2016 [2].

In this study, we used deterministic SIR model to understand COVID-19 dynamics in West African countries and estimated the overall number of susceptible individuals that accounted for 1.2% of West African population and 1% for most countries, except Guinea-Bissau, and Gambia where the susceptible individuals account for more than 9%. In general, small countries with relatively high population density are those with high proportion of susceptible individuals, indicating how high population density with small area can affect epidemics dynamics [57, 58]. Our findings however, revealed a great disparity between countries in terms of testing rate of COVID-19. Countries like Guinea and Gambia and in less extent, Côte d'Ivoire and Nigeria, showed a relatively less testing effort to identify many infected individuals. This suggests that there may not be enough tests being carried out to properly monitor the outbreak [55]. In contrast, countries like Cape-Verde, Benin and Togo, which have recorded less than or equal to 50 positive cases per 1,000 tests, seem to be effectively controlling the pandemic according to the WHO criteria [45]. Compared to relatively wealthier countries like Australia, South Korea and Uruguay, it takes hundreds of tests to find one case [55].

The detection rate considered in model (1) is a better indicator of testing effort since it represents the proportion of active cases in the population that are identified daily. Our results revealed a relatively low detection rate of COVID-19 in West Africa with less than 2% in most countries except Cape-Verde, Mauritania and Ghana ($> 5\%$). These three countries are also the ones with the highest testing rates (see table 1) confirming the link between detection rate and testing effort [5]. Thus, fairly low detection rates

in most West African countries demonstrate low testing effort and may be explained by a number of factors, including the availability of testing kits and qualified healthcare workers and low ability to control the disease due to their low GDP. For instance the average detection rate of COVID-19 in the world in April 2020 was estimated at 6% [59]. It is also useful to note that the estimated average detection rate hides a great variability in the testing effort over time. Indeed, it is generally accepted that the testing rate is relatively low at the very beginning of an epidemic outbreak but can increase rapidly over time when a better response mechanisms are put in place [60].

The dynamics of the COVID-19 pandemic in West Africa shows a reproduction number greater than 1 in all countries (from 1.2 in Burkina-Faso to 4.4 in Niger) while it was 1.4 for the whole region. This value is relatively low compared to that estimated by [24] (1.6) for the same region in June in a recent study using a modified SEIR model and thus reveals either a declining trend in the pandemic over time or the result of using a different modeling approach to estimate the reproduction number. The COVID-19 pandemic appears more serious than the Ebola outbreak in Africa given the basic reproduction number. Indeed, [8] estimated the basic reproduction number at 1.1, 1.2 and 1.2 for Guinea, Liberia and Sierra-Leone, respectively against 1.4, 1,3 and 1.6 for the same countries as far as COVID-19 is concerned. These comparisons indicate that COVID-19 is on average 1.29 times more reproducible than Ebola in these countries.

The trend in the running reproduction number reveals a rapid declining in all countries except Burkina-Faso and reveals some efficiency of the control measures put in place and being implemented in the different countries. Most countries have already experienced the peak in the new COVID-19 cases in June and July. In general, the reported peak was very low compared with the true peak.

However, current control measures should be maintained overtime to avoid possible second wave as observed in other parts of the world.

Conclusion

Our study shows that the novel COVID-19 pandemic, although highly contagious has not seriously impacted West Africa in terms of prevalence, compared to other parts of the world, in particular the Europe and the USA. Actually, the total number of susceptible

individuals and final epidemic size account for 1.2% and 0.6% of the total population size of West Africa, respectively. But the relatively low reported cases are related to very low testing effort in the West African countries. The study also indicates a relatively low detection rate and for most countries in the region, the dates of the true peak of infection have passed (June-July 2020). Nevertheless, the pandemic is still ongoing in the region and it is important that the non-pharmaceutical measures currently in place continue over time to help reduce its spread dynamics, pending adequate effective treatment.

Acknowledgments

HBT acknowledges the support of IMU-CDC through GRAID program. RGK acknowledges the support from the African German Network of Excellence in Sciences (AGNES) and the Alexander von Humboldt Foundation (AvH).

Authors' contributions

RGK conceived the ideas with SHH, designed the methodology, wrote the codes and supervised the work; SHH gathered the data, run the codes for some countries and wrote most sections of the manuscript; HBT run the codes for some countries and write some sections of the manuscript. All authors reviewed the drafts and gave final approval for publication.

Conflicts of Interest

The authors declares no conflict of interest.

References

1. Li J, Lou Y. Characteristics of an epidemic outbreak with a large initial infection size. J BIOL DYNAM. 2016;10(1):366–378.

2. Zhao S, Musa SS, Fu H, He D, Qin J. Simple framework for real-time forecast in a data-limited situation: the Zika virus (ZIKV) outbreaks in Brazil from 2015 to 2016 as an example. PARASITE VECTOR. 2016;10(1):366–378.

3. Wang XS, Wu J, Yang Y. RRichards model revisited: Validation by and application to infection dynamics. J THEOR BIOL. 2012;313:12–19.

4. Parodi A, Cozzani E. Coronavirus disease 2019 (COVID 19) and Malaria. Have anti glycoprotein antibodies a role?. MED HYPOTHESES. 2020.

5. Phipps S, Grafton RQ, Kompas T. Estimating the true (population) infection rate for COVID-19: A Backcasting Approach with Monte Carlo Methods. medRxiv preprint doi: `https://doi.org/10.1101/2020.05.12.20098889`. 2020.

6. Mendonça VR, Barral-Netto M. Immunoregulation in human malaria: the challenge of understanding asymptomatic infection. Mem Inst Oswaldo Cruz. 2015;110:945-–955.

7. Hsieh YH, Wu J, Fang J, Yang Y, Lou J. Quantification of bird-to-bird and bird-to-human infections during 2013 novel H7N9 avian influenza outbreak in China. PLoS One. 2014;9(12):e111834.

8. Wang XS, Zhong L. Ebola outbreak in West Africa: real-time estimation and multiple-wave prediction. arXiv preprint arXiv:1503.06908. 2015.

9. Dye C, Cheng RCH, Dagpunar JS, Williams BG. The scale and dynamics of COVID-19 epidemics across Europe. medRxiv 2020.06.26.20131144; doi: `https://doi.org/10.1101/2020.06.26.20131144`. 2020.

10. Hasan M, Hossain A, Bari W, Islam SS. Estimation of the basic reproduction number of novel coronavirus (COVID-19) in Bangladesh: A 65-day outbreak data-driven analysis. INFECT DIS-NOR. 2020;doi:10.21203/rs.3.rs-32412/v1.

11. Worldometer. African Countries by population (2020). `https://www.worldometers.info/population/countries-in-africa-by-population/` (Accessed on August 14, 2020).

12. Marimuthu S, Joy M, Malavika B, Nadaraj A, Asirvatham ES, Jeyaseelan L. Modelling of reproduction number for COVID-19 in India and high incidence states. CLIN EPIDEMIOL GLOBAL HEALTH. 2020.

13. Li Y, Wang LW, Peng ZH, Shen HB. Basic reproduction number and predicted trends of coronavirus disease 2019 epidemic in the mainland of China. INFECT DIS POVERTY. 2020;10(1):366–378.

14. Hsieh YH. Richards model: a simple procedure for real-time prediction of outbreak severity in *Modeling and dynamics of infectious diseases*. World Scientific; 2009;216–236.

15. Richards FJ. A flexible growth function for empirical use. J EXP BOT. 1959;10(2):290–301.

16. Weiss HH. The SIR model and the foundations of public health. Materials mathematics. 2013;01–17.

17. Magal P, Webb G. The parameter identification problem for SIR epidemic models: identifying unreported cases. J MATH BIOL. 2018;77(6-7):1629–1648.

18. He D, Gao D, Lou Y, Zhao S, Ruan S. A comparison study of Zika virus outbreaks in French Polynesia, Colombia and the State of Bahia in Brazil. Sci Rep. 2017;7:273.

19. Gao D, Lou Y, He D, Porco TC, Kuang Y, Chowell G, Ruan S. Prevention and control of Zika as a mosquito-borne and sexually transmitted disease: a mathematical modeling analysis. Sci Rep. 2016;6:28070.

20. Zhang Q, Sun K, Chinazzi M, Pastore y Piontti A, Dean NE, Rojas DP, Merler S, Mistry D, Poletti P, Rossi L, Bray M, Halloran ME, Longini Jr. IM, Vespignani A . Spread of Zika virus in the Americas. Proc Natl Acad Sci USA. 2017;114:E4334–43.

21. Towers S, Brauer F, Castillo-Chavez C, Falconar AK, Mubayi A, Romero- Vivas CM. Estimate of the reproduction number of the 2015 Zika virus outbreak in Barranquilla, Colombia, and estimation of the relative role of sexual transmission. Epidemics. 2016;17:50–55.

22. Brauer F, Castillo-Chavez C. Mathematical models in population biology and epidemiology. vol. 40. Berlin: Springer. 2016.

23. Lin Q, Chiu AP, Zhao S, He D. Modeling the spread of Middle East respiratory syndrome coronavirus in Saudi Arabia. Stat Methods Med Res. 2018; 27:1968–1978.

24. Taboe BH, Salako VK, Ngonghala CN, Tison J, Glèlè Kakaï R. Predicting COVID-19 spread in the face of control measures in West Africa. MATH BIOSCI, 2020; 328; 108431.

25. Djilali S, Ghanbari B. Coronavirus pandemic: A predictive analysis of the peak outbreak epidemic in South Africa, Turkey, and Brazil. CHAOS SOLITON FRACT. 2020;138.

26. Wynants L, Van Calster B, Collins GS, Riley RD, Heinze G, Schuit E, Bonten MMJ, Dahly DL, Darmen JAA, Debray TPA, de Jong VMT, De Vos M, Dhiman P, Haller MC, Harhay MO, Henckaerts L, Heus P, Kreuzberger N, Lohmann A, Luijken K, Ma J, Martin GP, Navarro CLA, Reitsma JB, Sergeant JC, Shi C, Skoetz N, Smits LJM, Snell KIE, Sperrin M, Spijker R, Steyerberg EW, Takada T, Tzoulaki I, van Kuijk SMJ, van Royen FS, Verbakel JY, Wllisch C, Wilkinson J, Wolff R, Hooft L, Moons KGM, van Smeden M. Prediction models for diagnosis and prognosis of covid-19 infection: systematic review and critical appraisal. BMJ-BRIT MED J. 2020;369:m1328.

27. Maleki M, Mahmoudi MR, Wraith D, Pho KH. Time series modelling to forecast the confirmed and recovered cases of COVID-19. TRAVEL MED INFECT DI. 2020;101742.

28. Sperrin M, Grant SW, Peek N. Prediction models for diagnosis and prognosis in Covid-19. BMJ-BRIT MED J Publishing Group.

29. Wangping J, Ke H, Yang S, Wenzhe C, Shengshu W, Shanshan Y, Jianwei W, Fuyin K, Penggang T, Jing L, Miao L, Yao H. Extended SIR prediction of the epidemics trend of COVID-19 in Italy and compared with Hunan, China. FRONT MED-LAUSANNE. 2020;7:169.

30. Wang L, Li J, Guo S, Xie N, Yao L, Cao Y, Day SW, Howard SC, Graff JC, Gu T, Ji J, Gu W, Sun D. Real-time estimation and prediction of mortality caused by COVID-19 with patient information based algorithm. SCI TOTAL ENVIRON. 2020;138394.

31. Anderson RM. Discussion: the Kermack-McKendrick epidemic threshold theorem. B MATH BIOL. 1991;53(1):1–32.

32. Zhang X, Ma R, Wang L. Predicting turning point, duration and attack rate of COVID-19 outbreaks in major Western countries. CHAOS SOLITON FRACT. 2020;109829.

33. He S, Tang S, Rong L. A discrete stochastic model of the COVID-19 outbreak: Forecast and control. Math Biosci Eng. 2020;17:2792–2804.

34. Martinez-Alvarez M, Jarde A, Usuf E, Brotherton H, Bittaye M, Samateh AL, Antonio M, Vives-Tomas J, D'Alessandro U, Roca A. COVID-19 pandemic in west Africa. LANCET GLOB HEALTH. 2020;18(5):e631–e632.

35. Holmes EA, O'Connor RC, Perry VH, Tracey I, Wessely S, Arseneault L, Ballard C, Christensen H, Silver RC, Everall I,Ford T, John A, Kabir T, King K, Madan I, Michie S, Przybylski AK, Shafran R, Sweeney A, Worthman CM. Multidisciplinary research priorities for the COVID-19 pandemic: a call for action for mental health science. LANCET PSYCHIAT. 2020.

36. Gilbert M, Pullano G, Pinotti F, Valdano E, Poletto C, Boëlle P-Y, d'Ortenzio E, Yazdanpanah Y, Eholie SP, Altmann M, Gutierrez B, Kraemer MUG, Colizza V. Preparedness and vulnerability of African countries against importations of COVID-19: a modelling study. LANCET. 2020;395(10227):871–877.

37. Nkengasong JN, Mankoula W. Looming threat of COVID-19 infection in Africa: act collectively, and fast. LANCET. 2020;395(10227):841–842.

38. El-Sadr WM, Justman J. Africa in the Path of Covid-19. NEW ENGL J MED. 2020.

39. Roda WC, Varughese MB, Han D, Li MY. Why is it difficult to accurately predict the COVID-19 epidemic?. INFECT DIS MODEL. 2020;5:271–281.

40. Anatassopoulou C, Russo L, Tsakris A, Siettos C. Data-Based Analysis, Modelling and Forecasting of the novel Coronavirus (2019-nCoV) outbreak. medRxiv. 2020.

41. Mizumoto K, Kagag K, Chowell G. Epidemiological and clinical features of the 2019 novel coronavirus outbreak in China. medRxiv. 2020.

42. Zahiri AP, Rafiee Nasab S, Roohi E. Prediction of Peak and Termination of Novel Coronavirus Covid-19 Epidemic in Iran. medRxiv. 2020.

43. Ma J. Estimating epidemic exponential growth rate and basic reproduction number. INFECT DIS MODEL. 2020;5:129–141.

44. WHO. Coronavirus disease (COVID-19): Situation Report – 208. `https://www.who.int/emergencies/diseases/novel-coronavirus-2019/situation-reports`. Accessed: 2020–08–15.

45. WHO. Public health criteria to adjust public health and social measures in the context of COVID-19. Annex to Considerations in adjusting public health and social measures in the context of COVID-19. 12 May, 2020.

46. WHO. Global health observatory data. 2020. `https://apps.who.int/gho/data/node.main.HWFGRP_0020?lang=en` (Accessed 10 April 2020).

47. Iwendi C, Bashir AK, Peshkar A, Sujatha R, Chatterjee JM, Pasupuleti S, Mishra R, Pillai S, Jo O. COVID-19 Patient Health Prediction Using Boosted Random Forest Algorithm. FRONT PUBLIC HEALTH. 2020;8:357.

48. Onovo A, Atobatele A, Kalaiwo A, Obanubi C, James E, Gado P, Odezugo G, Ogundehin D, Magaji D, Russell M. Using Supervised Machine Learning and Empirical Bayesian Kriging to reveal Correlates and Patterns of COVID-19 Disease outbreak in sub-Saharan Africa: Exploratory Data Analysis. Available at SSRN 3580721. 2020.

49. Tuli S, Tuli S, Verna R, Tuli R. Modelling for prediction of the spread and severity of COVID-19 and its association with socioeconomic factors and virus types. medRxiv. 2020.

50. Kucharski AJ, Russell TW, Diamond C, Liu Y, Edmunds J, Funk S, Eggo RM, Sun F, Jit M, Munday JD. Early dynamics of transmission and control of COVID-19: a mathematical modelling study. LANCET INFECT DIS. 2020. https://doi.org/10.1016/S1473-3099(20)30144-4.

51. Bizet NGC, Peña DKM. Time-dependent and time-independent SIR models applied to the COVID-19 outbreak in Argentina, Brazil, Colombia, Mexico and South Africa. arXiv preprint arXiv:2006.12479. 2020.

52. Tovissodé CF, Lokonon BE, Glèlè Kakaï R. On the use of growth models for forecasting epidemic outbreaks with application to COVID-19 data. medRxiv. 2020. https://www.medrxiv.org/content/early/2020/08/18/2020.08.16.20176057.

53. Pedersen MG, Meneghini M. Quantifying undetected COVID-19 cases and effects of containment measures in Italy. ResearchGate Preprint (online 21 March 2020) DOI. 2020.

54. Chowell G. Fitting dynamic models to epidemic outbreaks with quantified uncertainty: A primer for parameter uncertainty, identifiability, and forecasts. INFECT DIS MODEL. 2020;2(3):379–398.

55. Roser M, Ritchie H, Ortiz-Ospina E, Hasell J. Coronavirus Pandemic (COVID-19). Our World in Data (Accessed on August 20, 2020). 2020. https://ourworldindata.org/coronavirus.

56. MATLAB. Version 9.0.0 (R2016a). Computer Software, The MathWorks Inc., Natick, MA-USA. 2016.

57. Sumdani H, Frickle S, Le M, Tran M, Zaleta CK. Effects of Population Density on the Spread of Disease. Technical report 2014-05. 2014; The University of Texas Arlington, Mathematics Preprint Series, Texas, USA.

58. Sumdani H, Frickle S, Le M, Tran M, Zaleta CK. Effects of population density on the spread of disease. Complexity. 2001; 6(6): 29–36.

59. Bommer C, Vollmer S. Average detection rate of SARS-CoV-2 infections is estimated around six percent. Lancet Infect Dis. 2020.

60. Omori R, Mizumoto K, Chowell G. Changes in testing rates could mask the novel coronavirus disease (COVID-19) growth rate. INT J INFECT DIS. 2020; 94: 116–118.